POLITECNICO DI MILANO
Scuola di Ingegneria Industriale e dell'Informazione
Laurea magistrale in Ingegneria Matematica

3D Finite Element Drift-Diffusion Simulation of Semiconductor Devices

Relatore: Prof. Riccardo SACCO
Correlatore: Dott. Aurelio MAURI

Tesi di Laurea di:
Andrea BORTOLOSSI
Matr. n. 783023

Anno Accademico 2013–2014

Contents

List of Figures

List of Tables

Chapter 1

Post-Processing techniques for current density evaluation

In many physical and engineering problems the real interesting variable of the conservation law is the flux inside the domain. The study of micro and nano electronics devices does not except this observation so that an accurate good description of the current density is a basic requirement.

However, we recall that we chose to follow a displacement approach and this implies that the current density is not a dependent variable of the system rather, it is a post-processing quantity of computations.

In this chapter we investigate some techniques that allow us to reconstruct the current density inside the device, starting from the available model values of electric potential and carrier concentrations.

1.1 Drift-Diffusion formula

In Section **??** we saw that exist three different but mathematically equivalent ways to represent the current density, but due to numerical issues not all of them are appropriate for numerical implementation. In particular we exluded from our analysis the *Slotboom equations* (**??**)-(**??**) because the exponential dependency by the factor φ/V_{th} brings unavoidable numerical instability. The classical *Drift-Diffusion formula* (**??**)-(**??**) presents also some difficulties: the drift and diffusion contributions are respectively well defined but the combination of them may give rise oscillations.

Let us introduce some useful notation: with the subscript K we refer to a quantity defined on elements, while the subscript h refers to a quantity defined on vertices. The solutions φ_h, n_h and p_h obtained with the discretization scheme presented in Section **??** are piecewise linear continuous

functions over $\mathcal{T}_h$. According to (**??**) and (**??**), in order to compute $\mathbf{J}_n$ and $\mathbf{J}_p$ numerical differentiation of the solutions must be carried out. Notice that $\mathbf{J}_n, \mathbf{J}_p \in [X_h^0]^3$. If we want combine solutions and their derivatives, we have to compute appropriate projection of n_h and p_h

$$n|_K :=< n_h >$$
$$p|_K :=< p_h >$$

where with the symbol $< \cdot >$ we refer to a suitable average on the element, for example this operation could be the standard integral or the harmonic average presented in Section **??**. If the diffusion and the mobility coefficients are variable functions of the space and defined on vertices they also have to be projected on the space X_h^0.

We implemented a numerical differentiation based on Lagrange polynomial interpolation

$$\nabla n \simeq \nabla(\Pi_h^1 n) = \sum_{i=1}^{N_h} n_i \nabla \psi_i = \nabla n_h. \tag{1.1}$$

Notice that $\nabla n_h \in X_h^0$. The discretized form of equations (**??**), (**??**) reads as:

$$\mathbf{J}_n|_K = -qn|_K \mu_n \nabla \varphi_h + qD_n n|_K \nabla n_h \tag{1.2}$$
$$\mathbf{J}_p|_K = -qp|_K \mu_p \nabla \varphi_h - qD_p p|_K \nabla p_h \tag{1.3}$$

where for sake of simplicity we assume constant diffusion and mobility coefficients. Equations (1.2) and (1.3) can be easily computed over each element of $\mathcal{T}_h$.

1.2 Edge averaging techniques

It is well known that the classical Scharfetter-Gummel (SG) scheme for discretizing drift-diffusion models has proven itself to be the workhorse for semiconductor device modeling codes [GS69]. As a matter of fact the EAFE scheme proposed in Section **??** is strictly related to the FVSG (Finite Volume Scharfetter-Gummel) method presented by Bank, Fichtner and Rose [BRF83].

In this section we recall the Scharfetter-Gummel formula in a one-dimension spatial domain and we report the extension of the method to the 2D case proposed in [BCC98]. Finally we present a novel method in order to extend the Scharfetter-Gummel approach to the 3D framework.

1.2.1 The 1D Scharfetter-Gummel scheme

Consider the solution of the electron continuity equation along a one-dimensional domain. For sake of simplicity, we assume a uniform partition. Moreover at every node is defined the electrostatic potential φ_h, and in every element the associated electrostatic field $\mathbf{E}_K$.

In 1969 D. Scharfetter and H.K. Gummel (two scientists of Bell Labs), introduced a formula to compute the current density, in this case, given φ_h and the density solution (n_h) at each node of the discretization grid.

We know that the constitutive law is composed by a drift component, which depends on the electric field, and a diffusion component, which depends on the variation of the carrier density. Consider a generic element K and define the voltage drop $\Delta\varphi|_K = \varphi_{i+1} - \varphi_i$. There are three possible situations:

- $\Delta\varphi|_K \gg 0$, mainly drift component from right to left
- $\Delta\varphi|_K \ll 0$, mainly drift component from left to right
- $\Delta\varphi|_K \simeq 0$, mainly diffusion component

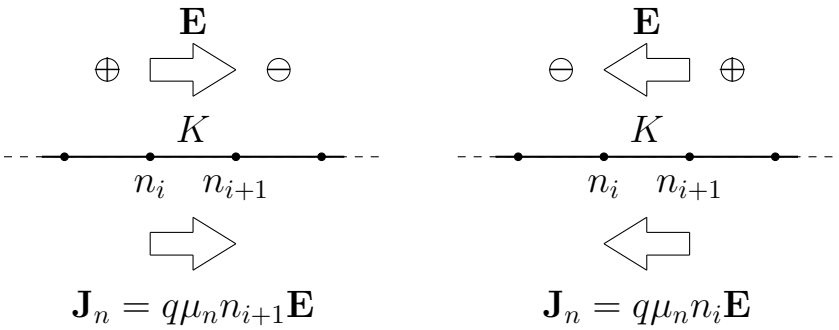

Figure 1.1: Effect of a high electric field over the current density of electron.

The three limiting situations can be accounted for by the following unifying SG formula

$$J_n|_K = q\frac{D_n}{h}\left[n_{i+1}\mathcal{B}\left(\frac{\Delta\varphi|_K}{V_{th}}\right) - n_i\mathcal{B}\left(-\frac{\Delta\varphi|_K}{V_{th}}\right)\right]. \tag{1.4}$$

In the case $\Delta\varphi|_K = 0$, the SG formula becomes

$$J_n|_K = qD_n\frac{n_{i+1} - n_i}{h} \tag{1.5}$$

which is the correct approximation of the current density using a $\mathbb{P}_1$ basis for n_h. When $\Delta\varphi|_K \gg 0$, the SG formula becomes

$$J_n|_K = q\mu_n n_i \frac{\Delta\varphi|_K}{h} \tag{1.6}$$

while for $\Delta\varphi|_K \ll 0$ we have

$$J_n|_K = q\mu_n n_{i+1} \frac{\Delta\varphi|_K}{h}. \tag{1.7}$$

The current density on the element K becomes similar to the Ohm's law where the carrier transported is n_{i+1} when $\Delta\varphi|_K \ll 0$ or n_i when $\Delta\varphi|_K \gg 0$. These situations are illustreated in Fig.1.1.

1.2.2 The 2D Scharfetter-Gummel scheme

One of the main results of [BCC98] is the equivalence between the finite volume and Galerkin discretizations of the continuity equation. In order to facilitate the connection between these two different discretization approaches the authors introduce for each $K \in \mathcal{T}_h$ a linear map $\mathcal{J}_K : \mathbb{R}^3 \to \mathbb{R}^2$ defined by

$$\mathcal{J}_K(\{\gamma_i\}_{i=1}^3) = \frac{1}{|K|} \sum_{i=1}^{3} \gamma_i |e_i| s_i \mathbf{t}_i \tag{1.8}$$

where s_i is the meausure of the segment from the midpoint of e_i to the intersection of the perpendicular edge bisectors and $\mathbf{t}_i$ denotes the unit tangent vector of the edge e_i. Fig.1.2 shows the parameters just presented. $\mathcal{J}_K$ has the following properties:

$$\mathcal{J}_K(\{\mathbf{J} \cdot \mathbf{t}_i\}_{i=1}^3) = \mathbf{J} \tag{1.9}$$

$$\mathcal{J}_K(\{s_i^{-1}\}_{i=1}^3) = 0 \tag{1.10}$$

$$\int_K \mathcal{J}_K(\{\gamma_i\}_{i=1}^3) \cdot \nabla\psi \, dK = \gamma_{i+1} s_{i+1} - \gamma_{i-1} s_{i-1}. \tag{1.11}$$

Equation (1.9) says that if we are able to compute the tangential component of the current density over all edges, we can combine these values according to (1.8) and obtain the current density $\forall K \in \mathcal{T}_h$.

For the EAFE scheme in the case of electron we have

$$\mathbf{J}_n \cdot \mathbf{t}_i = qD_n \frac{\mathcal{B}(\delta_i(\varphi_h/V_{th}))n_{h,k} - \mathcal{B}(-\delta_i(\varphi_h/V_{th}))n_{h,j}}{|e_i|} \tag{1.12}$$

where

$$\delta_i(\varphi_h/V_{th}) = \frac{\varphi_{h,k} - \varphi_{h,j}}{V_{th}}. \tag{1.13}$$

Similarly for the classical FVSG scheme this contribution is defined as

$$\mathbf{J}_n \cdot \mathbf{t}_i = \mathcal{H}_{e_i}(qD_n e^{\varphi_h/V_{th}})\nabla(\Pi^1|_K(e^{-\varphi_h/V_{th}} n_h)) \cdot \mathbf{t}_i \tag{1.14}$$

where $\mathcal{H}_{e_i}$ is the harmonic average along the edge e_i and $\Pi^1|_K$ is the interpolant over K. The extension of this procedure to the 3D case is non trivial, because the characterization of the cross-section s_i becomes more involved.

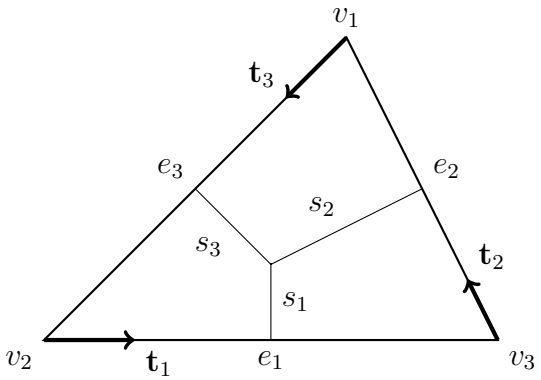

Figure 1.2: Parameters associated with element K.

1.2.3 The 3D Scharfetter-Gummel scheme

In this section we present novel method for the reconstruction of the electron current density over each element of the grid that is based on the so-called Primal-Mixed formulation [**?**].

We start by recalling here the formula for the electron current density expressed as a function of the quasi Fermi potential

$$\mathbf{J}_n = -q\mu_n n \nabla\varphi_n. \tag{1.15}$$

Relation (1.15) can be rewritten considering equation (**??**) as

$$\mathbf{J}_n \frac{\exp\left(\dfrac{\varphi_n - \varphi}{V_{th}}\right)}{q\mu_n n_i} + \nabla\varphi_n = 0. \tag{1.16}$$

Let $\mathbf{J}_n \in [L^2(\Omega)]^3$ and $\varphi_n, \varphi \in H^1(\Omega)$. We multiply (1.16) with a generic function $\mathbf{q} \in [L^2(\Omega)]^3$ and then intagrate over the domain Ω:

$$\int_\Omega \frac{\exp\left(\dfrac{\varphi_n - \varphi}{V_{th}}\right)}{q\mu_n n_i}\mathbf{J}_n \cdot \mathbf{q}\, d\Omega + \int_\Omega \nabla\varphi_n \cdot \mathbf{q}\, d\Omega = 0 \tag{1.17}$$

We proceed taking the usual discrete space of the piecewise constant functions over $\mathcal{T}_h$

$$V_h = \left\{ w \in L^2(\Omega) : w|_K \in \mathbb{P}_0 \forall K \in \tau_h \right\}. \tag{1.18}$$

Now the discrete quantities are $\mathbf{J}_n^h \in [V_h]^3$ and $\nabla\varphi_n^h \in V_h$. We consider the following choice of the test function $\mathbf{q}_h \in [V_h]^3$

$$\mathbf{q}_{1,2,3}^h = \left\{ \begin{bmatrix}1\\0\\0\end{bmatrix} \begin{bmatrix}0\\1\\0\end{bmatrix} \begin{bmatrix}0\\0\\1\end{bmatrix} \right\}. \tag{1.19}$$

From (1.17) we obtain a system of equations defined for each $K \in \mathcal{T}_h$:

$$\int_K \frac{\exp\left(\dfrac{\varphi_n - \varphi}{V_{th}}\right)}{q\mu_n n_i}\mathbf{J}_n^h \cdot \mathbf{q}_i^h\, dK + \int_K \nabla\varphi_n^h \cdot \mathbf{q}_i^h\, dK = 0 \qquad i = 1,2,3 \tag{1.20}$$

After intagration we obtain the formula for the generic component of the current density:

$$[\mathbf{J_n}]_i = -\mathcal{H}_K \left(q\mu_n n_i \exp\left(\frac{\varphi - \varphi_n}{V_{th}}\right)\right) \frac{\partial\varphi_n^h}{\partial x_i} \quad i = 1,2,3, \quad \forall K \in \tau_h \tag{1.21}$$

We do not evaluate the harmonic average with an exact 3D integration because it may be computationally expensive. Therefore, we approximate $\mathcal{H}_K(\cdot)$ by the following quadrature

$$\left(\frac{\int_K f^{-1}\, dK}{|K|}\right)^{-1} \simeq \left(\frac{\int_{e^*} f^{-1}\, de}{|e^*|}\right)^{-1} \tag{1.22}$$

where $f = q\mu_n n_i exp((\varphi - \varphi_n)/V_{th})$ and e^* is the edge of ∂K where the maximum drop of f occuring. The above idea amounts to assuming that the diffusion coefficient is represented by the edge where the phenomenon are more significant rather than considering the entire element. In order to define which is the correct edge, consider a quantity defined at the vertices

$$\Phi := \frac{\varphi - \varphi_n}{V_{th}} \tag{1.23}$$

which is the difference between the electrostatic potential and the quasi Fermi potential level. Now for every element consider two vertices: $\mathbf{x}_m$ s.t. $\Phi(\mathbf{x}_m) = \Phi_m := \min_K(\Phi)$ and $\mathbf{x}_M$ s.t. $\Phi(\mathbf{x}_M) = \Phi_M := \max_K(\Phi)$. Obviously it exists only one edge which connects these two points and on this one we perform the 1D integration (1.22).

Along the edge e^* we have

$$f(s) = q\mu_n n_i \exp\left(\Phi_m + (\Phi_M - \Phi_m)\frac{s - s_m}{|e^*|}\right) \tag{1.24}$$

where $s \in [s_m, s_M]$ is the parameter refered to the edge e^* s.t. $f(s_m) = f(\mathbf{x}_m)$ and $f(s_M) = f(\mathbf{x}_M)$. We can solve (1.22) with the following change of variables $\eta := (s - s_m)/|e^*|$ and proceed with trivial integration steps, to obtain

$$\begin{aligned}\int_{e^*} f^{-1}\, de &= |e^*| \int_0^1 \frac{\exp\left(-\Phi_m - (\Phi_M - \Phi_m)\eta\right)}{q\mu_n n_i}\, d\eta \\ &= |e^*| \frac{\exp(-\Phi_m)}{q\mu_n n_i} \frac{\exp(\Phi_m - \Phi_M) - 1}{\Phi_m - \Phi_M} \\ &= |e^*| \frac{\exp(-\Phi_m)}{q\mu_n n_i} \frac{1}{\mathcal{B}(\Phi_m - \Phi_M)}\end{aligned}$$

from which we finally get

$$\int_K f^{-1}\, dK \simeq q\mu_n n_i \exp(\Phi_m)\mathcal{B}(\Phi_m - \Phi_M). \tag{1.25}$$

Similar results may be obtained repeating the integration and considering s_M as starting point

$$\int_K f^{-1}\, dK \simeq q\mu_n n_i \exp(\Phi_M)\mathcal{B}(\Phi_M - \Phi_m). \tag{1.26}$$

Equation (1.25) and (1.26) can be combined to find

$$\mathbf{J}_n|_K = -q\mu_n \left[\frac{n_{\min}\mathcal{B}(-\Delta\Phi_{max}) + n_{\max}\mathcal{B}(\Delta\Phi_{max})}{2}\right] \nabla\varphi_n^h \tag{1.27}$$

where $n_{\min} = n_i e^{\Phi_m}$ and $n_{\max} = n_i e^{\Phi_M}$ while $\Delta\Phi_{\max} := \Phi_M - \Phi_m$. If we consider equation (1.27) over a one-dimensional domain we can recover equation (1.4), which shows that the above described approach is the natural extension of the $Scharfetter - Gummel$ formula to the 3D case.

1.3 Upwinding techniques

It is well known that the classical finite element method is unstable when the Pèclet number ($\mathbb{P}e$) is large. The coefficient $\mathbb{P}e$ includes the influence of the drift component and is proportional to the product $|\nabla\varphi|h$. Therefore the presence of boundary layers for the electrostatic potential makes the solution of the continuity equation a difficult task. This has led to the use of upwind finite element techniques: in the one-dimensional case this contribution is written as an artificial diffusion term which modifies the origin convection-diffusion equation. Generally speaking we can define a function $\Phi(\mathbb{P}e)$ of the Pèclet number such that

$$\lim_{\mathbb{P}e\to 0} \Phi(\mathbb{P}e) = 0. \tag{1.28}$$

The perturbed problem in the case of the electron continuity equation becomes

$$-\nabla\cdot(qD_n(1+\Phi(\mathbb{P}e))\nabla n - q\mu_n n\nabla\varphi) = -qR. \tag{1.29}$$

Similarly the new weak form is

$$a_h(n,v) = a(n,v) + \sum_{K\in\mathcal{T}_h}\int_K \Phi(\mathbb{P}e)\nabla n\cdot\nabla v\, dK. \tag{1.30}$$

Property (1.28) is fundamental in order to guarantee the consistency of (1.30) with respect to the standard Galerkin weak form.

Considering the framework just presented the *Scharfetter-Gummel* discretization scheme in one spatial dimension can be obtained using the following choice of the function Φ

$$\Phi(\mathbb{P}e) = \mathcal{B}(2\mathbb{P}e) + \mathbb{P}e - 1 \tag{1.31}$$

It is possible to deduce equation (1.31) considering (**??**) and (**??**) in some interesting limiting cases:

- **Constant carrier concentrations**, in the semiconductor device we have a current density due only to the drift contribution

$$\mathbf{J}_n = q\mu_n n\mathbf{E}$$
$$\mathbf{J}_p = q\mu_p p\mathbf{E}$$

- **Constant potential**, then we have $\mathbf{E} = 0$ and the current density is due only to the diffusive contribution

$$\mathbf{J}_n = qD_n\nabla n$$
$$\mathbf{J}_p = -qD_p\nabla p$$

- **Constant quasi Fermi potential**, then we have $n = C_1 e^{\varphi/V_{th}}$ and $p = C_2 e^{-\varphi/V_{th}}$ where C_1 and C_2 are two arbitrary constants such that

$$C_1 = \exp(-\bar{\varphi}_n/V_{th}) \qquad C_2 = \exp(\bar{\varphi}_p/V_{th})$$

where $\bar{\varphi}_n$ and $\bar{\varphi}_p$ are given contact values. Under this assumption from equations (**??**) and (**??**) we can enstablish that

$$\mathbf{J}_n = -q\mu_n(n\nabla\varphi - V_{th}(\frac{C_1}{V_{th}}\nabla\varphi e^{\varphi/V_{th}}) = 0$$
$$\mathbf{J}_p = -q\mu_p(p\nabla\varphi + V_{th}(-\frac{C_1}{V_{th}}\nabla\varphi e^{-\varphi/V_{th}}) = 0$$

which tells us that constant quasi Fermi potentials lead to thermodynamical equilibrium condition for the carrier densities and this implies no current flow in the device.

Consider the following modified version of (1.2) restricted to a single element K between two vertices (for the sake of simplicity we consider local indices for the vertices)

$$J_n|_K = -q\mu_n < n_h > \partial_x\varphi_h + qD_{n,h}\partial_x n_h \tag{1.32}$$

where:

$$D_{n,h} = (1 + \Phi_K(\mathbb{P}e))D_n$$
$$< n_h > = \frac{\int_K n_h\, dx}{|K|} = \frac{n_1 + n_2}{2}$$
$$\partial_x\varphi_h = \frac{\varphi_2 - \varphi_1}{h} = \frac{\Delta\varphi}{h}$$
$$\partial_x n_h = \frac{n_2 - n_1}{h}.$$

Equation (1.31) can be obtained imposing that

$$J_n|_K(\Pi_1^k(Ce^{\varphi/V_{th}})) = 0. \tag{1.33}$$

From (1.32) we have

$$\begin{aligned} q\mu_n < n_h > \partial_x\varphi_h &= qD_n(1+\Phi_K)\partial_x n_h \\ < n_h > \partial_x\varphi_h &= V_{th}(1+\Phi_K)\partial_x n_h \\ \Phi_K &= \sigma\mathbb{P}e\frac{n_1+n_2}{n_2-n_1} - 1 \end{aligned}$$

where

$$\begin{aligned} \mathbb{P}e &= \frac{\partial_x\varphi_h h}{2V_{th}} = \frac{\Delta\varphi}{2V_{th}} \\ \sigma &= sign(\Delta\varphi). \end{aligned}$$

Now we impose the constant quasi Fermi potential hypothesis

$$\begin{aligned} \Phi_K &= \sigma\mathbb{P}e\frac{e^{\varphi_1/V_{th}} + e^{\varphi_2/V_{th}}}{e^{\varphi_2/V_{th}} - e^{\varphi_1/V_{th}}} - 1 \\ &= \sigma\mathbb{P}e\frac{e^{\Delta\varphi/V_{th}} + 1}{e^{\Delta\varphi/V_{th}} - 1} - 1 \\ &= \sigma\mathbb{P}e\frac{e^{2\sigma\mathbb{P}e} + 1}{e^{2\sigma\mathbb{P}e} - 1} - 1. \end{aligned}$$

Setting $X := 2\sigma\mathbb{P}e$ we have

$$\begin{aligned} \Phi_K &= \frac{X}{2}\left(\frac{e^X}{e^X-1} + \frac{1}{e^X-1}\right) - 1 \\ &= \frac{1}{2}\left(\mathcal{B}(-X) + \mathcal{B}(X)\right) - 1 \\ &= \frac{1}{2}\left(X + \mathcal{B}(X) + \mathcal{B}(X)\right) - 1 \\ &= \mathcal{B}(X) + \frac{X}{2} - 1. \end{aligned}$$

Replacing the definition of X we obtain for both $\Delta\varphi > 0$ and $\Delta\varphi < 0$

$$\Phi_K = \mathcal{B}(2\mathbb{P}e) + \mathbb{P}e - 1. \tag{1.34}$$

From the above analysis we can say that a straightforward extension to the 3D case of the Scharfetter-Gummel stabilization can be found considering a 3×3 diagonal tensor $\underline{\underline{\mathbf{\Phi}}}^K$ defined on each element as follows

$$\underline{\underline{\mathbf{\Phi}}}^K_{ii} = -\frac{< \Pi_1^k(e^{\varphi/V_{th}}) > \partial_{x_i}\varphi}{\partial_{x_i}\Pi_1^k(e^{\varphi/V_{th}})V_{th}} - 1 \qquad i = 1,2,3, \tag{1.35}$$

In (1.36) the argument of the exponential can be a highly varying function over K, therefore it is preferable to consider a reference value for the electrostatic potential. Observe that $\varphi \in [\varphi_{min}, \varphi_{max}]$ and therefore we can use one of these values as reference and obtain

$$\underline{\underline{\mathbf{\Phi}}}^K_{ii} = -\frac{< \Pi_1^k(e^{(\varphi-\varphi_{min})/V_{th}}) > \partial_{x_i}\varphi}{\partial_{x_i}\Pi_1^k(e^{(\varphi-\varphi_{min})/V_{th}})V_{th}} - 1 \qquad i = 1,2,3, \tag{1.36}$$

1.3.1 Results

In this section we compare the performance of the different current computation methods . The test problems are the p-n junction (Tab.**??** $V_A = 1.0[V]$) and the n-MOSFET (Tab.**??** on-state condition). The procedures considered are:

- **Drift-Diffusion** defined by (1.2) and (1.3) with $n|_K = \mathcal{M}(n_h)$, where $\mathcal{M}(\cdot)$ is the standard integral average;
- **Scharfetter-Gummel 3D** method described in section 1.2.3;
- **Modified Drift-Diffusion** which is for the electron current density

$$\mathbf{J}_n|_K = -qn|_K\mu_n\nabla\varphi_h + qD_n n|_K(\underline{\underline{\mathcal{I}}} + \underline{\underline{\mathbf{\Phi}}}_K)\nabla n_h \tag{1.37}$$

  where $\underline{\underline{\mathcal{I}}}$ is the 3×3 identity tensor and considering $n|_K = \mathcal{M}(n_h)$ and $\underline{\underline{\mathbf{\Phi}}}_K$ as equation (1.36).

The comparison currents for the forward biased p-n junction are depicted in Fig.1.3 using 1D plots along a line parallel to the Z-axis and placed at the center of the device. Both electron and hole current densities are shown for the three methods. We note that the best result is obtained by the modified DD method, while the standard DD is unstable and the SG 3D computes wrong values of the current next to the contacts. Critical behaviour presented in Figs.1.3a and 1.3b are due to the wrong balance between drift and diffusion contributions, this problem is fixed by the upwinding technique as shown in Figs.1.3e and 1.3f.

The SG 3D scheme performs essentially well inside the device but considering the electron current density of Fig.1.3c we note incorrect behaviour at the contact where electrons are minority. (Fig.1.3d shows the dual effect for the holes). Physically speaking the current densities computed by the SG 3D formula are not wrong, indeed assuming ideal contacts we are enforcing that all the recombination of the excess carriers happens at the contact surface. This phenomena is well depicted by the boundary layers of the hole quasi Fermi potential presented in Fig.1.4a, moreover we note that as we refine the grid the behaviour is more bounded at contact and as a consequence we obtain a better prediction of $\mathbf{J}_p$ (Fig.1.4b).

The results for the n-MOSFET are shown in Fig.1.5 compared with SDEVICE (Fig.1.5a). The SG 3D scheme performs very well (Fig.1.5b). The most difficulty of the modified Drift-Diffusion scheme is the numerical evaluation of (1.36). When the current density presents a mainly component or equation (1.36) is far from critical computation (zero division or overflow) the upwinding scheme behaves very well. Considering more complex devices the above situations are not more valid and the results obtained are not good (Fig.1.5c). A better evaluation of (1.36) can be recovered using a finer mesh to the detriment of the computational cost. This test is shown in Fig.1.5d where we use a mesh with 35342 vertices (about ten times the number of degrees of freedom of the standard mesh). The result is not still good enough but comparing with the standard DD formula Fig.1.5e we appreciate a better behaviour.

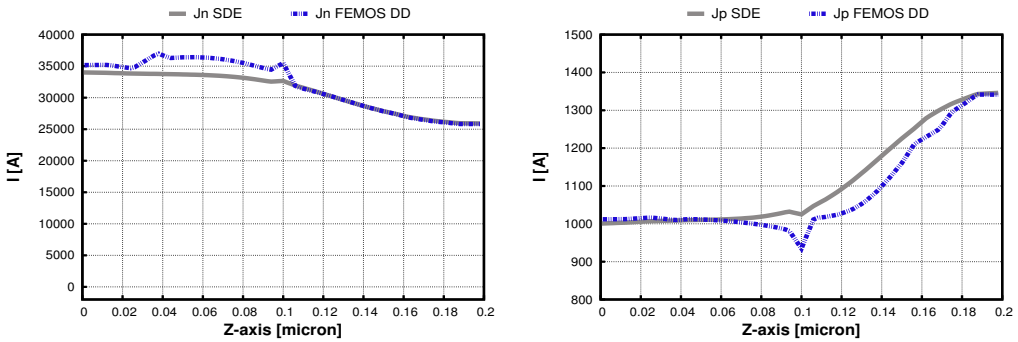

(a) *Standard DD - Jn*

(b) *Standard DD - Jp*

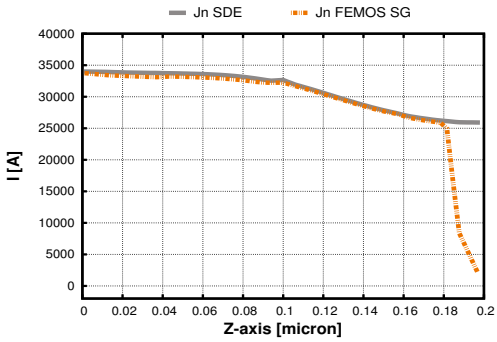

(c) *SG 3D - Jn*

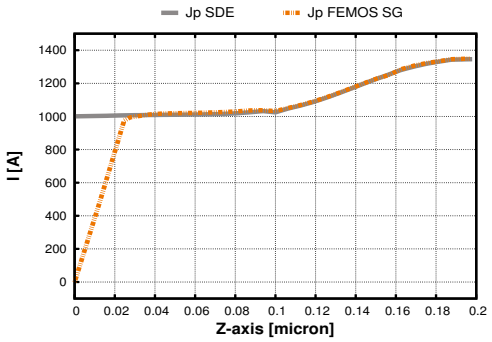

(d) *SG 3D - Jp*

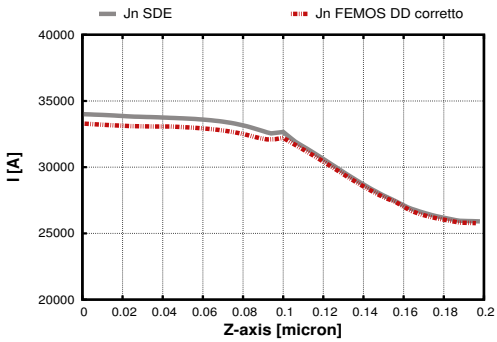

(e) *Modified DD - Jn*

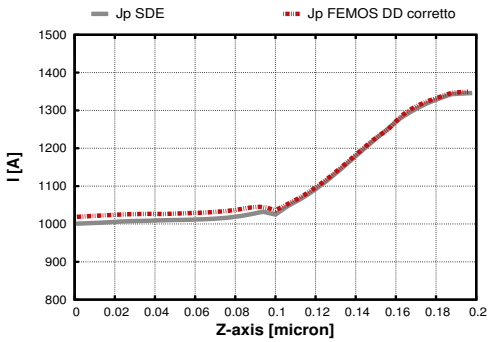

(f) *Modified DD - Jp*

Figure 1.3: 1D plot p-n junction - $V_A = 1.0[V]$

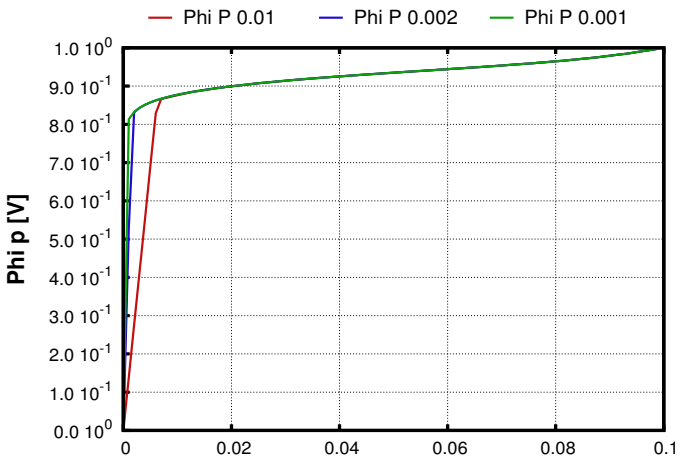

(a) *Hole quasi Fermi potential.*

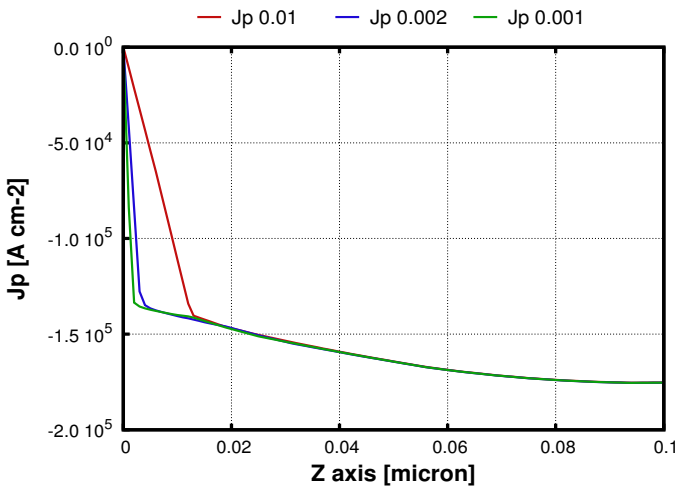

(b) *Jp.*

Figure 1.4: p-n junction forward biased - mesh refinement at contact

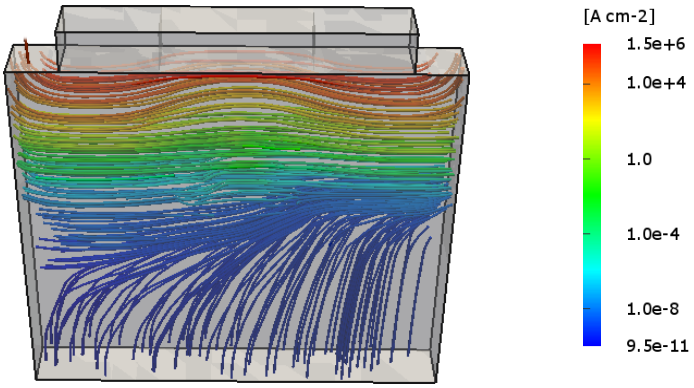

(a) *SDE*

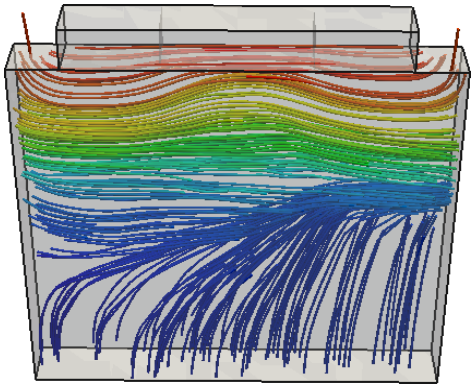

(b) *SG*

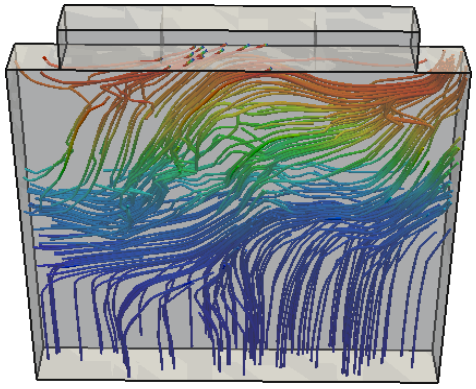

(c) *DD upwind*

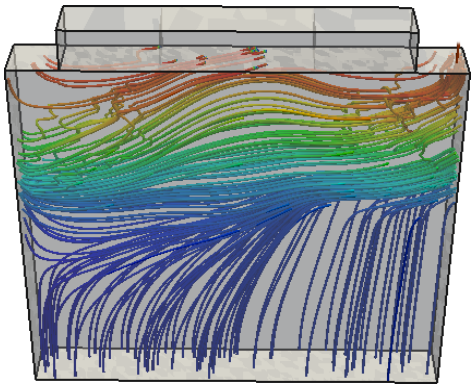

(d) *DD upwind (mesh finer)*

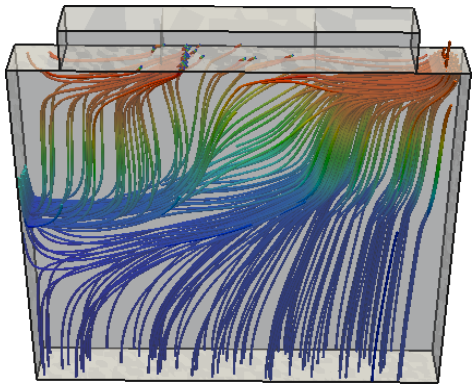

(e) *DD standard (mesh finer)*

Figure 1.5: n-MOSFET on-state - J_n.

Bibliography

[BCC98] R. E. Bank, W. M. Coughran, and L. C. Cowsar. The finite volume scharfetter-gummel method for steady convection diffusion equations. *Computing and Visualization in Science*, 1:123–136, 1998.

[BRF83] R. E. Bank, D. J. Rose, and W Fichtner. Numerical methods for semiconductor device simulation. *SIAM J. Sci. Stat.*, 4:416–514, 1983.

[GS69] H. K. Gummel and D. Scharfetter. Large-signal analysis of a silicon read diode oscillator. *IEEE Trans. Electron Devices*, pages 64–77, 1969.